Journal of Solid State Chemistry 182 (2009) 3226–3231

Contents lists available at ScienceDirect

Journal of Solid State Chemistry

journal homepage: www.elsevier.com/locate/jssc

Composition and structure of acid leached $LiMn_{2-y}Ti_yO_4$ $(0.2 \leq y \leq 1.5)$ spinels

Georgi Avdeev [b], José Manuel Amarilla [a], José María Rojo [a], Kostadin Petrov [b], Rosa María Rojas [a,*]

[a] Instituto de Ciencia de Materiales de Madrid, Consejo Superior de Investigaciones Científicas (CSIC), Sor Juana Inés de la Cruz no 3, Cantoblanco, 28049 Madrid, Spain
[b] Institute of General and Inorganic Chemistry, Bulgarian Academy of Sciences, 1113 Sofia, Bulgaria

ARTICLE INFO

Article history:
Received 17 June 2009
Received in revised form
2 September 2009
Accepted 14 September 2009
Available online 19 September 2009

Keywords:
Ti-doped $LiMn_2O_4$
Lithium manganese titanium oxide
Acid leaching
Oxide spinels

ABSTRACT

Lithium manganese titanium spinels, $LiMn_{2-y}Ti_yO_4$, $(0.2 \leq y \leq 1.5)$ have been synthesized by solid-state reaction between TiO_2 (anatase), Li_2CO_3 and $MnCO_3$. Li^+ was leached from the powdered reaction products by treatment in excess of 0.2 N HCl at 85 °C for 6 h, under reflux. The elemental composition of the acidic solution and solid residues of leaching has been determined by complexometric titration, atomic absorption spectroscopy and X-ray fluorescence analysis. Powder X-ray diffraction was used for structural characterization of the crystalline fraction of the solid residues. It has been found that the amount of Li^+ leached from $LiMn_{2-y}Ti_yO_4$ decreases monotonically with increasing y in the interval $0.2 \leq y \leq 1.0$ and abruptly drops to negligibly small values for $y > 1.0$. The content of Mn and Li in the liquid phase and of Mn and Ti in the solid (amorphous plus crystalline) residue, were related to the composition and cation distribution in the pristine compounds. A new formal chemical equation describing the process of leaching and a mechanism of the structural transformation undergone by the initial solids as a result of Li^+ removal has been proposed.

1. Introduction

Lithium manganese oxide spinel is very attractive cathode material for high-power applications; it has excellent rate capability due to its three-dimensional framework, and could offer low cost, long calendar life, and good safety characteristics. The substitution of several foreign cations for a part of manganese cations in pure $LiMn_2O_4$ has led to a notable improvement of its unsatisfactory 4 V cyclability, with only a marginal sacrifice of capacity [1]. Because of the excellent potential of the $LiM_yMn_{2-y}O_4$ (M=M^{2+}, M^{3+} and M^{4+} cations) compounds, the literature devoted to the study of different aspects of them is very copious. However, the low electrochemical performance of the Ti-doped materials [2–4] has considerably limited their studies. Some attention has been paid to compositions with very low dopant content [3,5–10], and some specific techniques have been applied to the structural characterization of some particular compositions [11–16]. We have recently synthesized and structurally characterized by powder X-ray diffraction (XRD) the solid solution formed in the $LiMn_{2-y}Ti_yO_4$ $(0.2 \leq y \leq 1.5)$ system [17]. Results provided from this characterization have been confirmed by studies of structural, magnetic and electrical properties carried on the title compounds in the compositional range $0 < y \leq 1$ [18].

The cation distribution in the cubic $LiMn_2O_4$ spinel (space group $Fd3m$) is described by the formula $(Li^+)[Mn^{3+}Mn^{4+}]O_4$, where symbols in parentheses and square brackets stand for cations occupying the tetrahedral ($8a$) and octahedral ($16d$) lattice sites of the spinel structure, respectively. When treated with diluted aqueous acid solutions, this compound converts to nearly pure spinel type manganese dioxide, (λ-Mn_2O_4) [19]. In the structure of this oxide, Mn^{4+} occupies the octahedral sites and the tetrahedral sites are vacant [20]. In contrast to this simple case, removal of lithium from substituted $LiMn_{2-y}M_yO_4$ spinels is more complex. The substituting cation M might have stable or variable oxidation-state. Its octahedral site preference energy might differ significantly from that of Mn^{3+} and Mn^{4+} and could cause redistribution of lithium over the spinel lattice sites. It might impede the electron hopping mobility, a prerequisite for the lithium removal [19]. Finally, it might be insoluble in the acid medium and segregated as a secondary residual solid.

Studies on the electrochemical properties of $LiMn_{2-y}M_yO_4$ (M=Ti, Ge, Fe, Zn and Ni), prior to and after leaching have been carried out. The observed changes in the elemental composition, lattice parameters, cations oxidation state and cations distribution within the spinel structure were nicely explained for M=Ge, Fe, Zn and Ni [2]. However, till now, models proposed to account for the poor electrochemical response of the Ti-doped compounds, and to

---

[*] Corresponding author. Fax: +34 91 3720623.
E-mail address: rmrojas@icmm.csic.es (R.M. Rojas).

0022-4596/$ - see front matter © 2009 Elsevier Inc. All rights reserved.
doi:10.1016/j.jssc.2009.09.009

describe quantitatively the Li-extraction are rather unsatisfactory. For $LiMn_{2-y}Ti_yO_4$ some questions concerning the structural transformations involved in the process of leaching are still open. Moreover, previous models about the random distribution of Mn^{3+} and Ti^{4+} in the (16*d*) sites [5,6], or partial occupancy of the tetrahedral (8*a*) sites by Li^+ and Ti^{4+} [11,13–15] are rather contradictory. They differ from the results reported by Petrov et al. [17] who, contrary to the existing concepts, propose for compositions with $y \leq 1.0$ a partial occupation of the tetrahedral (8*a*) by Mn^{2+}, while Li^+ is distributed over both tetrahedral (8*a*) and octahedral (16*d*) sites. It should be noted that mixed 1:1 occupation of the tetrahedral sites by Li^+ and M^{2+} has been found for a series of $LiM_{0.5}Ti_{1.5}O_4$ (M^{2+}=Co, Fe, Mg, Mn, Zn) with a primitive cubic lattice, space group $P4_332$, [17,21,22]. With this in mind and in view of the new structural model proposed [17] we have considered worthwhile to undertake a more detailed study on the phase composition and structure of the solid residue obtained by acid leaching $LiMn_{2-y}Ti_yO_4$ over an extended range of compositions ($0.2 \leq y \leq 1.5$). Analytical data for the elemental composition of both acid solutions and solid residues have been related to structural parameters of the initial compounds. Powder X-ray diffraction has been used to ascertain the phase transformations, composition and the most plausible cationic distribution of the crystalline part of the solid residues.

2. Experimental

2.1. Sample preparation

$LiMn_{2-y}Ti_yO_4$ ($0.2 \leq y \leq 1.5$) spinels were prepared by reacting, in air, stoichiometric mixtures of reagent grade Li_2CO_3, $MnCO_3$ and TiO_2 (anatase) carefully homogenized by grinding in agate mortar. Detailed description of the preparation procedure has been published elsewhere [17].

The powdered initial samples were reacted for 6 h, under reflux, in excess of 0.2 N HCl at 85 °C, with continuous stirring [23] and left overnight at room temperature to allow the suspended solid particles to settle down. The residual solids were separated from the liquid phase by filtering, washed with distilled water, and dried at 80 °C in air.

2.2. Chemical analysis

Lithium and manganese contents in the liquid phase were determined by atomic absorption spectroscopy (AAS). The manganese content was independently determined by complexometric titration. The Mn and Ti content in the solid residues after leaching were determined by X-ray fluorescence (XRF) analysis. XRF data for the untreated samples were used to set-up the calibration curves.

2.3. XRD measurements

Powder X-ray diffraction (XRD) data for phase identification and structural refinements were collected on a DRON automatic powder diffractometer, using Cu*K*α filtered radiation and Bragg-Brentano geometry. Step-scan data were recorded in the angle interval 10–115° (2θ) with a step of 0.02°(2θ) and a counting time of 4 s per step. Equal mass of powdered samples and identical sample holders were used in all measurements. Whole-pattern least-squares Rietveld refinements were carried out using the FULLPROF program suite [24]. Diffraction line profiles were approximated by pseudo-Voigt function. The refined instrumental and structural parameters were: zero-shift, scale factor, background parameters, unit cell parameter, half-width and mixing parameters, asymmetry parameters, atomic positional parameters, and individual isotropic displacement parameters. The site occupancies were constrained to the chemical analysis data. For samples with large *y*, the background was determined from manually selected experimental points. Site occupancies of the oxygen atoms were kept fixed to the spinel formula-unit content.

3. Results and discussion

3.1. X-ray diffraction results

XRD structural analysis has shown that the starting $LiMn_{2-y}Ti_yO_4$ samples have spinel type structure. Compounds whose composition falls within the interval $0.2 \leq y \leq 1.0$ crystallize in the space group *Fd*3*m*, with tetrahedral (8*a*) sites occupied by Li^+ and Mn^{2+}. The octahedral, (16*d*) sites are randomly occupied by Li^+, Mn^{3+}, Mn^{4+} and Ti^{4+}. The cation distribution is described by the approximate idealized formula $(L^{+}_{1-y/3}Mn^{2+}_{y/3})_{8a}[Li^{+}_{y/3}Mn^{3+}_{1-2y/3}Mn^{4+}_{1-2y/3}Ti^{4+}_{y}]_{16d}O_4$, which explains much better the observed oxygen parameters, bond lengths and bond valence sums (BVS) for the (8*a*) and (16*d*) sites [17,18], than the distribution allowing occupation of the (8*a*) sites by Li^+ and Ti^{4+} [23]. Compounds having $y > 1.0$ crystallize in the space group $P4_332$. The end member, $LiMn_{0.5}Ti_{1.5}O_4$ has lattice parameter a=8.4369(1) Å and cation distribution $(Li^{+}_{0.5}Mn^{2+}_{0.5})_{8c}[Li^{+}]_{4b}[Ti^{4+}_{1.5}]_{12d}O_4$. The tetrahedral (8*c*) sites have mixed (Li^+, Mn^{2+}) occupancy and the independent octahedral (4*b*) and (12*d*) sites are occupied by Li^+ and Ti^{4+}, respectively [17].

All patterns of the crystalline phase in the leached $0.2 \leq y \leq 1.0$ samples were indexed with a face centered cubic lattice, space group *Fd*3*m*, while those having $y > 1.0$ were indexed with a primitive cubic lattice, space group $P4_332$. The XRD pattern of pristine $LiMnTiO_4$, y=1, sample is shown in Fig. 1a, and patterns recorded for $LiMn_{2-y}Ti_yO_4$, (y=0.2, 0.4, 1) samples after leaching are plotted as an example in Fig. 1b, c and d, respectively. On increasing *y* (Fig. 1.) the diffraction profiles become broader. This is an indication of small crystallite size and probably of compositional micro-deformations common for products obtained by leaching. Moreover, in the range 22–35° (2θ) an anomalous background is also observed. It was ascribed to diffuse scattering from an amorphous phase, whose relative content gradually increases with *y*. This fact indicates that after leaching Li^+ a secondary amorphous phase is formed. At the experimental condition given, the dopant cation Ti^{4+} does not form soluble compounds. It is plausible then to assume that it partly segregates from the pristine material as an amorphous oxide or oxide-hydroxyde phase. The lattice parameter of the samples prior to and after leaching vs. Ti content, *y*, has been plotted in Fig. 2. For $0.2 \leq y \leq 1.0$, the lattice parameter of the leached samples is significantly smaller than the parameters of the pristine compounds. This result agrees with that reported by Tarascon et al. for the compositional range $0 \leq y \leq 1$ [2]. It can be accounted for assuming that as a result of Li^+ removal, the Mn^{3+} ions in the solid oxidizes to Mn^{4+} whose ionic radius is much smaller than those of Mn^{2+} and Mn^{3+} present in the pristine compounds. In the compositional range $0.2 \leq y \leq 1$ the dependence of lattice parameter on *y*, prior to and after leaching shows practically the same slope (Fig. 2). However, the lattice parameters of the leached samples show an abrupt increase between y=1 and 1.2. For $1.2 \leq y \leq 1.5$ the leached and the pristine samples have practically identical lattice parameters, being this results an indication that Li^+ has not been extracted from samples within this compositional interval.

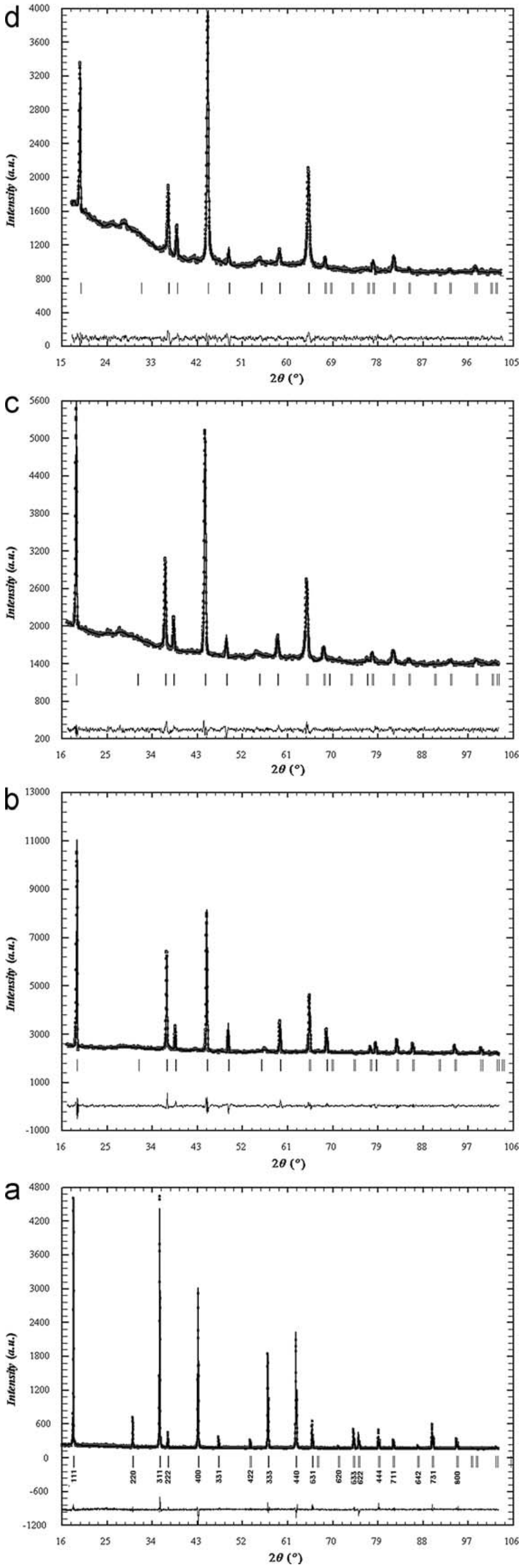

Fig. 1. XRD patterns of: pristine $LiMnTiO_4$ (a), leached $LiMn_{2-y}Ti_yO_4$, $y=0.2$ (b), $y=0.4$ (c), $y=1.0$ (d).

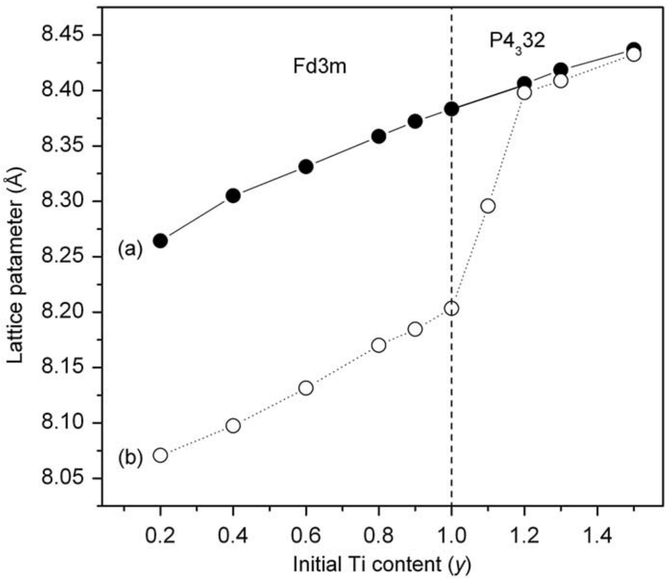

Fig. 2. Lattice parameters of $LiMn_{2-y}Ti_yO_4$, $(0.2 \leq y \leq 1.5)$ vs. y, prior to (closed symbols ●) and after leaching (open symbols ○).

3.2. *Elemental composition of acid liquid and solid residue after leaching*

According to Hunter [19], the extraction of Li^+ from $LiMn_2O_4$ by acid leaching is described by the formal equation:

$$2LiMn_2O_{4Solid} = 2Li^+_{(aq)} + Mn^{2+}_{(aq)} + 1.5\lambda\text{-}Mn_2O_{4solid} \qquad (1)$$

the atomic ratio Li/Mn in the solution being equal to 2. The mechanism of delithiation involves: (i) disproportionation of some Mn^{3+} of the surface of the pristine material ($2Mn^{3+}=Mn^{2+}+Mn^{4+}$); (ii) dissolution of the resulting Mn^{2+} and Li^+ in the acid medium; (iii) diffusion of Li^+ ions from the bulk to the surface of the solid $LiMn_2O_4$, this process being accompanied by (iv) electron hopping from donor Mn^{3+} in the bulk to acceptor Mn^{4+} on the surface. Thus the insoluble Mn^{4+} from the surface transforms to Mn^{3+} that can disproportionate again. The process continues until all the lithium is removed from the pristine material and all remaining manganese ions in the residual solid are transformed to Mn^{4+} [19]. Theoretical results obtained from first principles thermodynamic studies brought valuable information on the driving force of the process and the role of Mn^{3+} disproportionation in the dissolution reaction [25].

Assuming that all the Li^+ could be removed from the pristine solid, the formal equation of leaching for the $LiMn_{2-y}Ti_yO_4$ spinel should be

$$2LiMn_{2-y}Ti_yO_{4solid} \rightarrow 2Li^+_{(aq)} + Mn^{2+}_{(aq)} + 3/2(Mn_{2(3-2y)/3}Ti_{4y/3}O_4)_{Solid} \qquad (2)$$

It would maintain the Li/Mn atomic ratio of the solution constant and equal to 2, but the Ti/Mn atomic ratio for the solid residue, $2y/(3-2y)$, would depend on y.

The chemical analyses have shown that the liquid phase obtained after the acid treatment of the $LiMn_{2-y}Ti_yO_4$, $0.2 \leq y \leq 1.5$, samples was practically free of Ti^{4+}, and contained only Mn^{2+} and Li^+ cations. The analytical results are summarized in Table 1 and Fig. 3. It can be seen that for samples at $0.2 \leq y \leq 1$ the amount of dissolved Li^+ and Mn^{2+} decreases monotonically with increasing y, the Li/Mn ionic ratio being close to 2. The last fact indicates that for the mentioned interval of y the mechanism of Hunter would hold [19], however, the formal chemical description of the process would be different from Eqs. (1) and (2).

Table 1
Analytical results of the acid liquid phase, and of the solid fractions obtained after leaching $LiMn_{2-y}Ti_yO_4$ ($0.2 \leq y \leq 1.5$) spinels.

Ti content y in $LiMn_{2-y}Ti_yO_4$	Ions extracted from 1 mole $LiMn_{2-y}Ti_yO_4$ (liquid phase)		Composition of the solid residue determined by XRF				
			Composition (g/100 g)		Atomic ratio (Ti/Mn)		
	Li^+	Mn^{2+}	Ti	Mn	Calculated for the initial spinel	Determined for the solid residue	Calculated from Eq. (5)
0.2	0.960	0.465	6.0	53.8	0.11	0.13	0.15
0.4	0.905	0.449	13.8	46.7	0.25	0.34	0.34
0.6	0.861	0.401	21.6	39.5	0.43	0.63	0.60
0.8	0.828	0.381	28.9	32.9	0.67	1.01	0.96
0.9	0.806	0.366	31.0	28.5	0.82	1.25	1.20
1	0.773	0.339	34.0	25.4	1.0	1.54	1.50
1.1	0.601	0.324	36.2	23.8	1.22	1.74	
1.2	0.201	0.113	38.1	21.5	1.50	2.03	
1.3	0.080	0.030	39.7	19.3	1.86	2.36	
1.5	0.020	0.010	42.3	16.1	3.0	3.00	

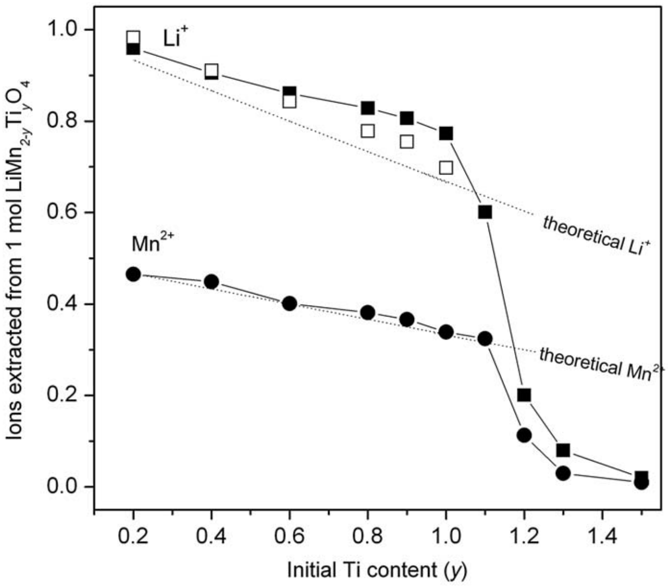

Fig. 3. Ions leached from 1 mole $LiMn_{2-y}Ti_yO4$ ($0.2 \leq y \leq 1.5$): experimental values (closed symbols ●, ■); theoretical values ($Li^+=3-y/3$) and ($Mn^{2+}=3-y/6$) according to Eq. (5) (dotted lines); and Li^+ (8*a*) site occupancy determined from XRD for the initial compounds (open symbol □) [17].

For samples at $y > 1$ the amount of dissolved Li^+ and Mn^{2+} drops, and finally neither Li^+ nor Mn^{2+} are practically leached from the composition $LiMn_{0.5}Ti_{1.5}O_4$. Similar result has been reported for $LiM_{0.5}Ti_{1.5}O_4$ and $LiM_{0.5}Ge_{1.5}O_4$ (M=Cu, Co, Mg, Zn) spinels which do not deintercalate Li^+ electrochemically due to the lack of long-range electronic conduction [21].

Results obtained from the XRF analysis of solid residues after acid leaching are also summarized in Table 1. As seen, the atomic Ti/Mn ratio determined for each composition is systematically higher than the calculated for the corresponding starting compound, i.e. the residual solid becomes enriched in insoluble Ti-bearing products.

Acid leaching of $LiMn_{2-y}M_yO_4$ (M=Ti, Ge, Fe, Zn or Ni) spinels has been systematically treated by Tarascon et al. [2]. The authors proposed a simple and reliable solution for dopants with permanent or variable oxidation state which are soluble in acidic medium. However, the case of insoluble dopants still requires further precision. For example, leaching of spinel doped with insoluble tetravalent cation, like Ti^{4+}, was described by the equation [2]:

$$2(2-y)LiMn_{2-y}Ti_yO_4+4(2-y)H^+ \rightarrow 2(2-y)Li^+ +(2-y)Mn^{2+}+ yTiO_2+(3-2y)Mn_{2-y}Ti_yO_4+2(2-y)H_2O \quad (3)$$

Here, like in Eq. (1) and (2), the atomic Li/Mn ratio of dissolved Li^+ and Mn^{2+} equals 2.0, but now some titanium oxidic phase segregates from the octahedral sites of the spinel as TiO_2. According to Eq. (3), all Li^+ is leached out of the spinel while the present and other reported results [2,23] indicate fractional extraction of Li^+. To the best of our knowledge no satisfactory even qualitative explanation has been given for this fact. Based on the capacity loss observed on discharging leached Ti-doped spinels Tarascon et al. [2] suggested that insoluble amorphous TiO_2 phase deposited on the surface of the spinel upon leaching, obstructs the insertion/removal of lithium. The explanation, however, has not been definitely confirmed by other studies; in contrast, it has been reported that TiO_2-coated $LiMn_2O_4$ cathode material exhibits better cyclic performance that the uncoated one in different potential regions [26,27].

We propose, as an alternative, a semi-empirical approach which could explains the partial removal of Li^+ from $LiTi_yMn_{2-y}O_4$, giving at the same time information about the chemical composition of the crystalline residue. Let us assume that leaching is predetermined by the proposed cation distribution for the pristine spinels: $(Li^+_{1-y/3}Mn^{2+}_{y/3})_{8a}[Li^+_{y/3}Mn^{3+}_{1-2y/3}Mn^{4+}_{1-2y/3}Ti^{4+}_y]_{(16d)}O_4$ [17]. The window formed by three nearest oxygen atoms of the $Li_{(8a)}$ occupied tetrahedral has a free diameter of 0.94–0.99 Å, while the free diameter of the triangular window of the $Li_{(16d)}$ occupied octahedra is much smaller, 0.52–0.57 Å. Thus, bulk migration is allowed for the $(Li)_{8a}$ only, while $(Li)_{16d}$ remains trapped due to the "bottleneck effect". Therefore, the amount of lithium leached, $(Li)_L$, from one formula unit should be equal to the number of lithium ions occupying the (8*a*) sites of the pristine spinel, i.e. $(Li^+)_L=(3-y)/3$. The equivalent amount of dissolved manganese, $(Mn^{2+})_L$, is $(Mn^{2+})_L=(Li)_L/2=(3-y)/6$. When dissolving Mn an equiproportional amount of titanium, $(Ti)_S$, should segregate from the solid, i.e.:

$$(Mn^{2+})_L/(2-y)=(Ti)_S/y \text{ or } (Ti)_S=y(3-y)/6(2-y) \quad (4)$$

Now Eq. (3) may be rewritten as

$$LiMn_{2-y}Ti_yO_4=(3-y)/6Li_2O_{dissolved}+ (3-y)/6MnO_{dissolved}+y(3-y)/6(2-y)TiO_{2segregated}+ [Li_{y/3}Mn_{(9-5y)/6}Ti_{y(9-5y)/6(2-y)}O_{2(9-5y)/3(2-y)}]_{crystalline\ residue} \quad (5)$$

The amounts of leached lithium $(Li^+)_L$ and manganese $(Mn^{2+})_L$ are known from the chemical analyses (see Table 1). Then the amount of segregated $(Ti^{4+})_S$ can be calculated from Eq. (4). If $(Li^+)_L$, $(Mn^{2+})_L$ and $(Ti^{4+})_S$ are known, then the total amount of their oxygen counterpart ($\sum O$) can be calculated. Hence the contents of Li, Mn, Ti and O in the crystalline $LiMn_{2-y}Ti_yO_4$ residue can be calculated as follows: $Li=1-(Li^+)_L$; $Mn=(2-y)-(Mn^{2+})_L$, $Ti=y-(Ti^{4+})_S$, and $O=4-\sum O$.

The theoretical amounts $(Li^+)_L$ and $(Mn^{2+})_L$ leached from one mole $LiMn_{2-y}Ti_yO_4$ according to Eq. (5) are plotted against y in Fig. 3. as straight dotted lines. The corresponding experimental values (Table 1), are given as closed symbols in the same plot.

It can be seen that the experimental values for $(Mn^{2+})_L$ agree well with those calculated from Eq. (5). The experimental values for $(Li^+)_L$, however, are systematically higher, the maximum value being 0.78 for $y=1$ and decreasing for $y<1$. This value is consistent with the value of 0.79 determined by other authors [23]. So, leaching of excess Li^+ using boiling acid solution seems to be a real effect.

The excess of leached Li^+ could be due to several factors: (i) ion exchange between Li^+ from the solid and H^+ from the acidic solution during leaching; (ii) dissolution of an additional fraction of Li^+ from the (16*d*) sites, which accompanies Ti^{4+} segregation from same sites; and (iii) the pristine spinels might contain more tetrahedral Li than the predicted by the theoretical model [17]. This effect is shown by the open symbols in Fig. 3. Whatever are the reasons, the experimental data show qualitatively that the amount of Li extracted decreases almost linearly on increasing y with the slope of $\approx 1/3$. This slope is predicted by both the theoretical cation distribution already proposed [17], and by that proposed in Eq. (5).

3.3. *Structural analysis of the crystalline residue*

The starting model for Rietveld refinement was a defect spinel $Li_{2y(2-y)/(9-5y)}Mn_{2-y}Ti_yO_4$ which composition was deduced after normalization of the last right term of Eq. (5) against a spinel formula unit. Refinement results for several solid residues with $0.2\le y\le 1.0$ are summarized in Table 2. Typical Rietveld plots are shown in Fig. 1b–d. The plot of pristine $LiMnTiO_4$ (Fig. 1a) has been added for comparison.

Table 2
Refined structural parameters and reliability factors for the crystalline residues of leached $LiMn_{2-y}Ti_yO_4$ spinels, S.G. *Fd*3*m*.

Atom	Site	SOF	B_{iso} (Å^2)
$y=0.2$; $a=8.0707(4)$ (Å); R_{wp}: 2.56; R_{exp}: 2.05; χ^2: 1.56; R_B: 2.14			
Li	16*d*: (1/2, 1/2, 1/2)	0.046	0.50(4)
Ti		0.100	
Mn		0.854(6)	
Mn	16*c*: (0, 0, 0)	0.046(6)	0.61(5)
O	32*e*: (*u*, *u*, *u*) *u*=0.2548(3)	1.000	1.3(2)
$y=0.4$; $a=8.0974(3)$ (Å); R_{wp}: 2.51; R_{exp}: 2.27; χ^2: 1.22; R_B: 2.79			
Li	16*d*: (1/2, 1/2, 1/2)	0.066	0.53(5)
Ti		0.200	
Mn		0.692(7)	
Mn	16*c*: (0, 0, 0)	0.108(7)	0.68(6)
O	32*e*: (*u*, *u*, *u*) *u*=0.2545(3)	1.000	1.4(2)
$y=0.6$; $a=8.1315(8)$ (Å); R_{wp}: 2.67; R_{exp}: 2.49; χ^2: 1.15; R_B: 1.51			
Li	16*d*: (1/2, 1/2, 1/2)	0.099	0.72(4)
Ti		0.300	
Mn		0.522(7)	
Mn	16*c*: (0, 0, 0)	0.185(7)	0.76(5)
O	32*e*: (*u*, *u*, *u*) *u*=0.2533(3)	1.000	1.7(2)
$y=0.8$; $a=8.1701(6)$ (Å); R_{wp}: 3.00; R_{exp}: 2.78; χ^2: 1.17; R_B: 1.71			
Li	16*d*: (1/2, 1/2, 1/2)	0.128	0.66(8)
Ti		0.400	
Mn		0.399(6)	
Mn	16*c*: (0, 0, 0)	0.209(6)	0.74(8)
O	32*e*: (*u*,*u*,*u*) *u*=0.2526(3)	1.000	1.6(3)
$y=1.0$; $a=8.2033(9)$ (Å); R_{wp}: 3.17; R_{exp}: 3.04; χ^2: 1.09; R_B: 1.28			
Li	16*d*: (1/2, 1/2, 1/2)	0.175	0.81(6)
Ti		0.500	
Mn		0.280(8)	
Mn	16*c*: (0, 0, 0)	0.229(8)	0.84(7)
O	32*e*: (*u*, *u*, *u*) *u*=0.2509(3)	1.000	1.8(2)

In contrast to the pristine materials, several diffraction peaks like (220), (422) etc., in the patterns of the leached samples at $0.2\le y\le 1.0$ are unobserved. Hence, occupation of the tetrahedral (8*a*) sites by some "heavy", Mn and/or Ti, atoms with high X-ray scattering factors is unlikely. These sites should be occupied either by "light" Li atoms or should be vacant. Patterns simulated by placing all Li atoms in (8*a*) and the rest of the "heavy" atoms in (16*d*) positions, did not show the drastic change observed in the relative intensities of the experimental patterns on increasing *y*. Due to the small X-ray atomic scattering factor of Li, all calculated diagrams looked much the same, like that recorded for the leached sample with $y=0.2$ (see Fig. 2b.). Therefore, since the (8*a*) sites should be vacant, all cations would be placed at the octahedral positions. Since for $y>0$ the number of cations for the $Li_{2y(2-y)/(9-5y)}Mn_{2-y}Ti_yO_4$ formula unit is greater than two, part of them should be placed in the (16*c*) sites. Pattern simulations with this model distribution reproduced the observed drastic change of intensities, provided the (16*c*) sites are occupied predominantly by "heavy" atoms. With increasing *y*, a strong increase in the intensity of some selected diffraction peaks, such as (222), (400) and (440), accompanied by a decrease in the intensity of the (111) and (311) peaks was observed (Fig. 1). That is why, a cationic distribution $[Mn_z]_{16c}[Li_xMn_{2-y-z}Ti_y]_{16d}O_4$ was ascribed to the starting structural model of the solid residue. Ti and Li atoms retained the (16*d*) sites like in the pristine compounds, and their site occupancy was constrained to the composition determined from chemical analysis. The site occupancy factor, *z*, for the (16*c*) sites was included as a variable parameter, constraining the total Mn amount to chemical analysis data. The values of the refined parameters are summarized in Table 2. Refinement ended with satisfactory values of the statistical criteria for the fit (Table 2). For the leached samples, the lattice parameter increases linearly with increasing *y* from 0.2 to 1.0. The oxygen parameter *u* decreases, tending to the ideal value of $u=0.250$. The refined parameters show definitely that the crystal structure of the residual phases, especially those with relatively high *y* values, do not belong to the λ-MnO_2 structural type. In the structure of λ-MnO_2 the metal atoms occupy only the octahedral (16*d*) sites, whereas in the crystalline residue the 3*d*-metal ions are distributed over (16*c*) and (16*d*) octahedral sites. Both sites are partly vacant, the fraction of (16*c*) vacancies being much higher. The diffraction patterns gave no evidences for cation ordering. This cation distribution seems to be directly related to both the cation distribution in the pristine compounds and the mechanism of leaching. Topologically, a similar structure was ascribed to the solid residue obtained from leached $LiMnTiO_4$ [23]. In this study, the authors assumed occupation of the (16*c*) sites by Ti^{4+}.

In contrast to $LiMn_2O_4$, $LiMn_{2-y}Ti_yO_4$ contains Mn^{2+}, Mn^{3+} and Mn^{4+}. Hence, electron hopping from bulk Mn^{2+} to surface Mn^{4+} or Mn^{3+} cannot be ruled out. The spatial distribution of occupied lattice sites in the spinel structure is shown as $\langle 111\rangle$ projection of a fraction of two adjacent polyhedral layers in Fig. 4. The lower one is built of occupied octahedra, arranged in a kagomé pattern. The upper one is built of occupied tetrahedra and octahedra. Li^+ and the high-spin state $Mn^{2+}(3d^5)$, whose octahedral site preference energy is zero, occupy the tetrahedral sites randomly. If removal of Li^+ is accompanied by electron

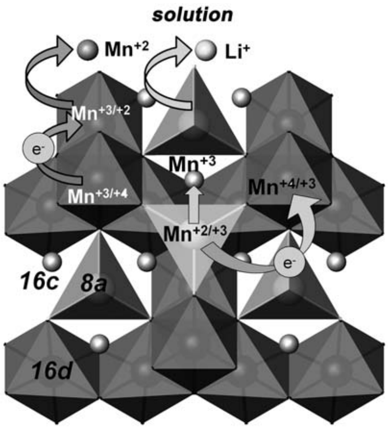

Fig. 4. Schematic representation of the acid leaching of $LiMn_{2-y}Ti_yO_4$ ($0.2 \leq y \leq 1.0$). Top left: $2(Mn^{3+})_{16d}=(Mn^{4+})_{16d}+(Mn^{2+})_{16d}$ and Mn^{2+} dissolution. Top middle: $(Mn^{2+})_{8a}+(Mn^{4+})_{16d}=(Mn^{3+})_{16d}+(Mn^{3+})_{16c}$ and shifting of $(Mn^{3+})_{8a}$ to a vacant (16*c*) site.

hopping from a bulk Mn^{2+} to a surface Mn^{4+}, both ions transform to $Mn^{3+}(3d^4)$ (recombination, see top middle part of Fig. 4). The octahedral site preference energy of Mn^{3+} is very high, 95.3 kJmol^{-1} [28]. Therefore, it should shift from the tetrahedral (8*a*) site to the adjacent, energetically more favorable, vacant octahedral (16*c*) site, as shown by the straight vertical arrow in Fig. 4. The shift results in a structure which may be regarded as a defect spinel whose kagomé layers are separated not by a "mixed" layer of (8*a*) tetrahedra and (16*d*) octahedra, but by a partly vacant layer of (16*c*) and (16*d*) octahedra. Thus, the occupation of the (8*a*) tetrahedral sites by Mn^{2+} ions, and the physical reason for their migration to the vacant octahedral (16*c*) upon oxidation to Mn^{3+}, finds its argumentation.

4. Conclusions

Series of $LiMn_{2-y}Ti_yO_4$, ($0.2 \leq y \leq 1.5$) spinels have been synthesized and leached with diluted hot HCl acid. The distribution of Li, Mn and Ti between the acidic liquid, the amorphous Ti-containing phase and a residual crystalline lithium titanium oxide phase has been studied by chemical analysis, XRF and powder XRD analysis.

The results from data processing have shown that the composition and the structure of the reaction products are strongly dependent on the cation distribution in the starting compound. The primitive $P4_332$ spinels ($1.0 < y \leq 1.5$) are stable against leaching, probably due to their low electronic conduction which is a requirement for Li^+ removal. In contrast, Li^+ is readily removed from $Fd3m$ ($0.2 \leq y \leq 1.0$) spinels. The amount of removed Li^+ decreases linearly with a slope of $\approx 1/3$, on increasing *y*, as expected from the tetrahedral site occupancy $(1-y/3)$ in the pristine compounds. A new formal chemical equation for the process of leaching $LiMn_{2-y}Ti_yO_4$ ($0.2 \leq y \leq 1.0$) has been proposed. It accounts for the observed amount of leached-Li^+, for the amount of segregated amorphous Ti-containing phase and for the composition of the crystalline residue. The latter is essential for the choice of a realistic starting model for structural refinement. Results from the refinement indicate that the crystalline residue has a defect type spinel structure whose (8*a*) sites are vacant and (16*d*) and (16*c*) sites are partly occupied. The occupation of the (16*c*) sites gradually increases with increasing *y*. This fact looks rather exceptional in comparison with numerous reported cation deficient spinels containing vacancies in (8*a*), (16*d*) or in both sites.

Acknowledgments

Financial support through project MAT 2008-03182 (MICINN), and the joint project CSIC-Bulgarian Academy of Sciences no. 2007BG0018 is gratefully recognized.

References

[1] L. Guohua, H. Ikuta, T. Uchida, M. Wakihara, J. Electrochem. Soc. 143 (1996) 178–182.
[2] J.M. Tarascon, E. Wang, F.K. Shokoohi, W.R. McKinnon, S. Colson, J. Electrochem. Soc. 138 (1991) 2859–2864.
[3] Y. Shao-Horn, R.L. Middaugh, Solid State Ionics 139 (2001) 13–25.
[4] G. Perentzis, E.E. Horopanitis, L. Papadimitriou, Ionics 12 (2006) 269–274.
[5] G. Kumar, H. Schlorb, D. Rahner, Mater. Chem. Phys. 70 (2001) 117–123.
[6] K. Soo Yoo, N. Woong Cho, Y.-J. Oh, Solid State Ionics 113–115 (1998) 43–49.
[7] L. Hernán, J. Morales, L. Sánchez, J. Santos, Solid State Ionics 118 (1999) 179–185.
[8] Y. Shin, A. Manthiram, J. Electrochem. Soc. 151 (2004) A204–A208.
[9] C. Bellito, E.M. Bauer, G. Righini, M.A. Green, W.R. Branford, A. Antonini, M. Pasquali, J. Phys. Chem. Solids 65 (2004) 29–37.
[10] L. Zhang, T. Yabu, I. Taniguchi, Mater. Res. Bull. 44 (2009) 707–713.
[11] S. Suzuki, M. Tomita, S. Okada, H. Arai, J. Phys. Chem. Solids 57 (1996) 1851–1856.
[12] B. Ammundsen, M.S. Islam, D.J. Jones, J. Roziére, J. Power Sources 81 (1999) 500–504.
[13] P. Strobel, A. Ibarra-Palos, M. Anne, C. Poinsignon, A. Crisci, Solid State Sci. 5 (2003) 1009–1018.
[14] M.A. Arillo, M.L. López, C. Pico, M.L. Veiga, A. Jiménez-López, E. Rodriguez-Castellón, J. Alloys Compds. 317–318 (2001) 160–163.
[15] M.A. Arillo, G. Cuello, M.L. López, P. Martín, C. Pico, M.L. Veiga, Solid State Sci. 7 (2005) 25–32.
[16] Q.H. Wu, J.M. Xu, Q.Ch. Zhuang, S.G. Sun, Solid State Ionics 177 (2006) 1483–1488.
[17] K. Petrov, R.M. Rojas, P.J. Alonso, J.M. Amarilla, M.G. Lazarraga, J.M. Rojo, Solid Sate Sci. 7 (2005) 277–286.
[18] N. Krins, F. Hatert, K. Traina, L. Dusoulier, I. Molenberg, J.F. Fagnard, Ph. Vanderbemden, A. Rulmot, R. Cloots, B. Vertruyen, Solid State Ionics 177 (2006) 1033–1040.
[19] J.C. Hunter, J. Solid State Chem. 39 (1981) 142–147.
[20] J.E. Greedan, N.P. Raju, A.S. Willis, C. Morin, S.M. Shaw, J.N. Reimers, Chem. Mater. 10 (1998) 3058–3067.
[21] H. Kawai, M. Tabuchi, M. Nagata, H. Tukamoto, A.R. West, J. Mater. Chem. 8 (1998) 1273–1280.
[22] G. Avdeev, K. Petrov, I. Mitov, Solid State Sci. 9 (2007) 1135–1139.
[23] B. Krutzsch, E. Kemmler-Sack, J. Less-Comm. Met. 124 (1986) 111–123.
[24] J. Rodriguez-Carvajal, Physica B (Amsterdam) 192 (1993) 55–69.
[25] R. Benedek, M.M. Thackeray, Electrochem. Solid-State Lett. 9 (2006) A265–A267.
[26] Z. Zhang, Z. Gong, Y. Yang, J. Phys. Chem. 108 (2004) 17546–17552.
[27] L. Yu, X. Qiu, J. Xi, W. Zhu, L. Chen, Electrochim. Acta 51 (2006) 6406–6411.
[28] J.D. Dunitz, L.E. Orgel, Adv. Inorg. Radiochem. 2 (1960) 1–60.